

Biosensing on Digital Microfluidics: From Sample Preparation to Detection

Ehsan Samiei and Mina Hoorfar

1 Introduction

In recent years, the tendency to adopt digital microfluidics (DMF) for lab-on-a-chip (LOC) applications has increased extensively. This is due to the unique advantages that DMF offers comparing to other microfluidic systems. Many analytical and physical techniques for performing biochemical experiments have been reconfigured to be compatible with DMF systems, and numerous studies have shown the use of DMF technology for different biochemical applications. Along with the progress made towards the development of liquid handling and sample preparation aspects, biochemical detection techniques have continuously been reconfigured to be compatible with DMF chips, and nowadays, multiple DMF-based devices are developed with integrated detection systems for real-time- or on-line biosensing and diagnosis purposes.

This chapter briefly introduces DMF, along with detection techniques which have been integrated into these devices. Then, the development of the sample preparation techniques for DMF systems is discussed in detail. Finally, the applications of DMF platforms with integrated detection systems used in different biochemical applications are discussed.

E. Samiei · M. Hoorfar (✉)
University of British Columbia, 3333 University Way, Kelowna,
BC V1V 1V7, Canada
e-mail: mina.hoorfar@ubc.ca

© Springer International Publishing AG 2018
S.-H. Oh et al. (eds.), *Miniature Fluidic Devices for Rapid Biological Detection*,
Integrated Analytical Systems, https://doi.org/10.1007/978-3-319-64747-0_7

2 Digital Microfluidics (DMF)

Miniaturized devices such as lab-on-a-chip (LOC), introduced for downscaling and automating biochemical processes, have attracted a significant attention in the past decades. LOC offers numerous advantages over the conventional in-laboratory methods used in performing biochemical experiments. These advantages include, but not limited to automation, low consumption of samples and reagents, high surface-to-volume ratio resulting high reaction rates, low manpower and human error, and high control on sample manipulation [1]. Microfluidics is the key to the development of LOC devices, as the manipulation of the samples is performed with microfluidic systems. The primary microfluidic systems introduced include permanently etched microchannels through which liquid sample flows using different pumping mechanisms. In the past two decades, digital microfluidic (DMF) platforms have been introduced which function based on the manipulation of liquid samples in the form of droplets in pico-liter to microliter sizes. The discrete nature of sample manipulation and control on individual droplets on DMF offers multiple advantages: (i) a single chip can be programmed for different applications using one design of actuating electrodes; and (ii) the sample volume dispensed can be controlled with high accuracy; (iii) numerous droplets can be manipulated simultaneously, allowing for parallel and high throughput operations. Due to these features, DMF has been widely used for LOC applications. Many researchers have focused on the advancement of the operators on DMF for performing different processes; while other groups have implemented these operators for biochemical applications. Among different operators developed and used in many applications is biosensing. Different biosensing mechanisms have been integrated into DMF for off-chip and on-chip detection. This section briefly explains the DMF technology and the biosensing mechanisms integrated to these devices.

2.1 Droplet Actuation Mechanisms

Unlike the droplet microfluidics in which the sample droplets are formed and transported in a continuous flow of a carrier liquid, the droplets on DMF devices are manipulated individually on an array of electrodes. The array of electrodes could be designed in a 2D configuration, allowing for the transport of droplets in different directions on the planar chip surface. Such a configuration makes DMF versatile and reconfigurable for different applications, since the droplet path can be programmed depending on the application on demand.

Droplet manipulation on DMF devices has been performed through several mechanisms, relying on surface and body forces applied on the liquid. These mechanisms include thermocapillary [2, 3], magnetic force [4, 5], surface acoustic

wave [6, 7], dielectrophoresis (DEP) [8, 9], electrowetting-on-dielectric (EWOD) [10, 11], and optoelectrowetting [12, 13]. Although all of these mechanisms have shown to be functional in terms of droplet manipulation, EWOD is the most effective and widely used method in DMF devices. Thus, among the different methods, only the principal of EWOD is explained here.

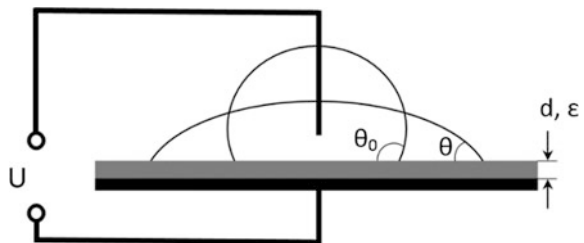
2.1.1 Electrowetting-on-Dielectric

Electrowetting-on-dielectric was developed by Berge in early 1990s based on the electrocapillarity (electrowetting) effect which was introduced by Gabriel Lippmann in 1875 [14]. In electrowetting, when a conductive liquid is in contact with an electrode and a voltage is applied between them, the liquid spreads on the surface. This may result in a change in the apparent contact angle formed between the liquid and the substrate. Lippmann’s electrowetting experiment was performed using mercury and an electrolyte. However, aqueous solutions are subject to electrolytic decomposition when the applied voltage is higher than a few hundred millivolts. Berge solved this problem by placing an insulating layer between the liquid and the electrode, introducing electrowetting-on-dielectric (EWOD) [14]. This phenomenon is schematically shown in Fig. 1 where the contact angle before and after applying voltage (U) is θ_0 and θ , respectively. Due to the application of the voltage, electrons and counter-ions will be accumulated in the interface of the insulating layer and the liquid, and therefore, a force will be applied to the three-phase contact line (TPCL), pulling TPCL and changing the apparent contact angle. The horizontal force and also the change in the apparent contact angle depends on the magnitude of the applied voltage, i.e., the higher the voltage, the higher the force. However, the change in the apparent contact angle is limited to a certain value (referred to as the saturation contact angle), above which the angle remains unchanged even with the application of a higher voltage.

Lippmann-Young equation (Eq. 1) is a simple correlation between the applied voltage and the change in the contact angle [15]

$$\cos\theta = \cos\theta_0 + \frac{1}{2} \frac{C}{\sigma_{lv}} U^2, \tag{1}$$

Fig. 1 Schematic of the electrowetting-on-dielectric (EWOD) phenomenon



where C and σ_{lv} are the capacitance of the insulating layer and the liquid–vapor interfacial tension, respectively. This equation, however, is valid only for a low range of the applied voltage. The results deviate from the experimental values when the contact angle is close to the saturation contact angle [15, 16]. Berthier et al. [15, 16] developed a more complicated correlation which was accurate even for higher applied voltages

$$\frac{\cos\theta - \cos\theta_0}{\cos\theta_S - \cos\theta_0} = \coth\left(\frac{3CU^2}{2\sigma_{lv}(\cos\theta_S - \cos\theta_0)}\right) - \frac{1}{\frac{3CU^2}{2\sigma_{lv}(\cos\theta_S - \cos\theta_0)}} \quad (2)$$

In this equation θ_S is the saturation contact angle.

EWOD also exerts a force on the droplet. Several approaches have been developed to formulate the EWOD force. Here, electromechanical approach, which is the most accurate method in estimating the EWOD force, is briefly presented. With some simplifications [14], the stress acting on an infinitesimal element of liquid due to an electric field (generated by the applied voltage to the system (Fig. 1)) can be presented using Maxwell stress tensor [14]

$$T_{ik} = \epsilon_0 \epsilon \left(E_i E_k - \frac{1}{2} \delta_{ik} E^2 \right), \quad (3)$$

where ϵ_0 , ϵ are the permittivity of vacuum and the insulating layer, respectively, δ_{ik} is the Kronecker delta function, E is the electric field and $i, k = x, y$ and z . The force acting on the liquid can be calculated using the following equation:

$$F_i = \oint T_{ik} n_k dA, \quad (4)$$

where n is the unit normal vector to the liquid–vapor interface and dA is the area of an infinitesimal element at the interface. After integration and considering certain assumptions (the details can be found in [14, 17]) the horizontal component of the EWOD force per unit area can be calculated as

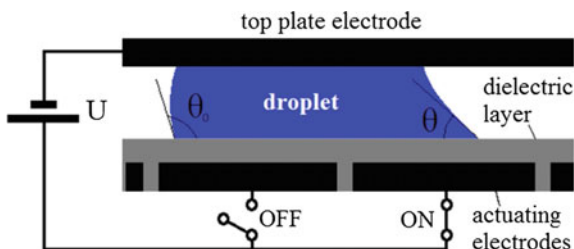
$$F_x = \frac{\epsilon_0 \epsilon}{2d} U^2, \quad (5)$$

where d is the thickness of the insulating layer.

2.1.2 EWOD Actuation on DMF

As explained earlier, EWOD is the common mechanism used for droplet manipulation on DMF devices. In order to transport a droplet on the chip, the EWOD force has to be applied to the droplet asymmetrically. For this purpose, the electrode on the surface is divided to multiple smaller electrodes, electrically addressable

Fig. 2 Schematic of a typical DMF device



individually. In addition, the wire in Fig. 1 is replaced with a top plate coated with a metal layer. Figure 2 illustrates the schematic of a DMF device which consists of (i) a bottom layer containing the actuating electrodes and covered by the insulating layer, (ii) the top plate containing the ground electrode, and (iii) the liquid droplet sandwiched between the two plates. To transport a droplet on the chip, the chip surface has to be hydrophobic. Therefore, a thin hydrophobic layer is coated on both bottom and top plates.

2.1.3 Open and Closed DMF Systems

In the previous section, it was shown that in order to use EWOD for transporting a droplet on the chip, the top wire was replaced with a top plate containing an electrode. This configuration is called the “closed” or “sandwiched” system (Fig. 3a). However, that is not the only configuration that could be used for such a purpose. The ground electrode could also be patterned on the bottom plate, beside the actuating electrode. This configuration does not need a top plate and is referred to as the “open” system (Fig. 3b). The open system allows for simple liquid dispensing methods (such as pipetting) on to the chip, and has been used in multiple studies [18, 19]. However, it is not as common as the closed system since in the case of the open systems, the evaporation rate is high and droplet manipulation is not as straightforward as the closed system [1].

2.1.4 Basic Fluidic Operations

Performing biochemical experiments on the chip requires generating specific volumes of different samples and reagents, transporting the liquid volumes, and mixing them to reach a uniform mixture. On DMF devices, these operations are performed by applying EWOD using the patterned electrodes on the bottom plate. Transport of droplets on the chip is carried out by sequential actuation of the electrodes. As shown in Fig. 4a, when the adjacent electrode to the droplet is actuated, EWOD pulls the droplet towards the electrode; when it wets the entire electrode surface, the

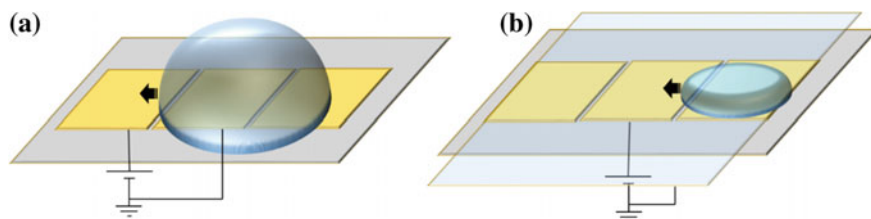


Fig. 3 Schematic of **a** open, and **b** closed (sandwiched) DMF systems

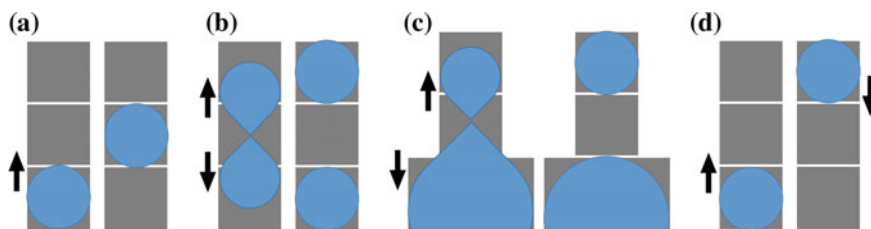


Fig. 4 Basic fluidic operations on DMF devices: **a** transport, **b** splitting, **c** dispensing, and **d** mixing

next electrode will be actuated to maintain the transport process. This is the basis of droplet transport on DMF which was introduced in [10].

Generating a specific volume of samples is performed by splitting a bigger droplet (referred to as mother droplet) into two smaller droplets (referred to as daughter droplets) or extracting a small droplet from a larger droplet in the reservoir. The former is called splitting and the latter is referred to as dispensing. To split a mother droplet into two daughter droplets, normally three electrodes are required. First the droplet is transported to the middle electrode, and then by actuating the two side electrodes (while the middle one is turned off) the droplet is split (Fig. 4b). Dispensing is also very similar to splitting. The droplet is pulled on the array of electrodes from the reservoir electrode to form a liquid finger, and then the reservoir and the second actuating electrode will be actuated to dispense a small droplet (Fig. 4c).

Mixing is also an important operation required for biochemical applications where more than one sample or component is involved. When two sample droplets are merged, due to the high aspect ratio of the droplet (diameter-to-height ratio) the content will not be mixed properly. Several methods have been developed in order to achieve proper mixing inside the droplet, which will be discussed in detail in Sect. 3. Here the basic mixing method is shown in Fig. 4d. In essence, it involves transport of the droplet back and forth on an array of three or four electrodes until the content is mixed properly.

2.2 *Detection Systems Integrated into DMF Systems*

Biosensing or detection is a key process and probably the final step in biochemical experiments, as after the sample preparation is carried out on the device, the final product is taken to the sensing component to detect a specific analyte [1]. Historically, right after the development of fluidic operations, DMF devices were used for performing biochemical assays which included detection. In early studies, the DMF devices were used only for a part of or the entire sample preparation step, and the product was taken off the chip and delivered to the detection device which was mainly fluorescence microscopy [20]. This mode of sensing is referred to as off-line sensing. The tendency to develop DMF-based LOC platforms for point-of-care applications (in which the entire assay process is required to be performed on the chip) resulted in the integration of the biosensors into DMF devices. Such a mode of sensing is referred to as online sensing, where the biosensing component is a part of the DMF chip. Several sensing mechanisms integrated into DMF devices will be discussed in this section.

2.2.1 **Optical Systems**

Optical detection systems widely coupled with DMF devices include absorbance, fluorescence, chemiluminescence, and surface plasmon resonance (SPR) detection systems [1, 20]. Absorbance techniques [21, 22] are based on UV/Vis absorption spectroscopy which works based on the measurement of the attenuation of the incident light in a range of the wavelengths. The part of the spectrum in which the attenuation peaks depends on the type of the analyte, which is used for the identification of the specific analytes that are present in the sample.

In fluorescence detection techniques [23, 24], the target analyte is labeled using a fluorescent dye. The fluorescence detection systems include a light source for excitation, and a fluorescent photodetector for detecting the signal. The fluorescent labels are excited using a high-intensity light source, and upon excitation, they emit low intensity, long wavelength light which is detected using a fluorescent detector (microscope, spectrometer, or well-plate reader).

Chemiluminescence [25, 26] techniques are conceptually similar to the fluorescence techniques in a way that the light emitted from the labeled analyte is detected. However, in chemiluminescence system, a chemical reaction occurs between the target analyte and an enzyme label instead of using a fluorescent dye and an exciting light source. This method is very sensitive and selective and its application is more straightforward as it is based on a chemical reaction and only requires the integration of a photodetector for detecting the signal [20].

Surface plasmon resonance (SPR) [27, 28] is a sensitive, label-free optical detection technique which is based on the measurement of the change in the

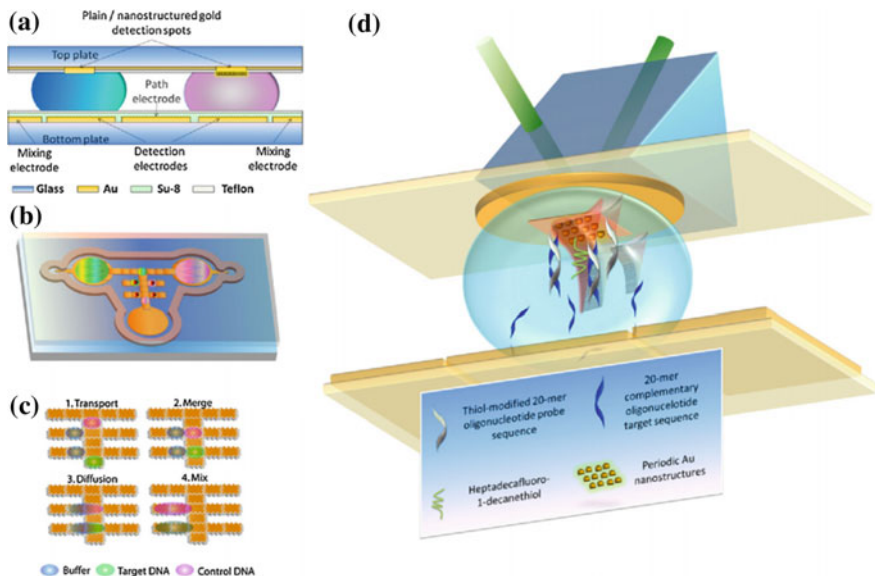


Fig. 5 Schematic of a DMF chip with integrated surface plasmon resonance (SPR) detection system. Reproduced from [28] with permission from Elsevier

refractive index of the reflected light from a light beam shined to the surface of the sensor through a prism. The SPR biosensor consists of a thin metal layer in contact with the liquid sample and a dielectric layer which is usually a prism. The frequency of the light source is adjusted with the natural frequency of the surface plasmon formed at the metal–dielectric interface. The refractive index of the reflected light is measured using a photodetector. As the target biochemical analytes bind to the receptors on the metal layer, the refractive index of the reflected light changes. A schematic of SPR biosensor integrated into a DMF platform is illustrated in Fig. 5.

2.2.2 Mass Spectrometry

Mass spectrometry is an analytical method which has been coupled with DMF for biosensing purposes. This method functions based on sorting the chemical species within the sample into a spectrum is dependent on the mass-to-charge ratio of the species [29]. The equipment used for mass spectrometry is large, and therefore, it is not feasible to miniaturize and integrate the device into the DMF chip [20]. Instead, these systems are interfaced with the DMF chips, normally using microscale tubes, to transfer the sample from the chip to the spectrometer [29]. Figure 6 shows

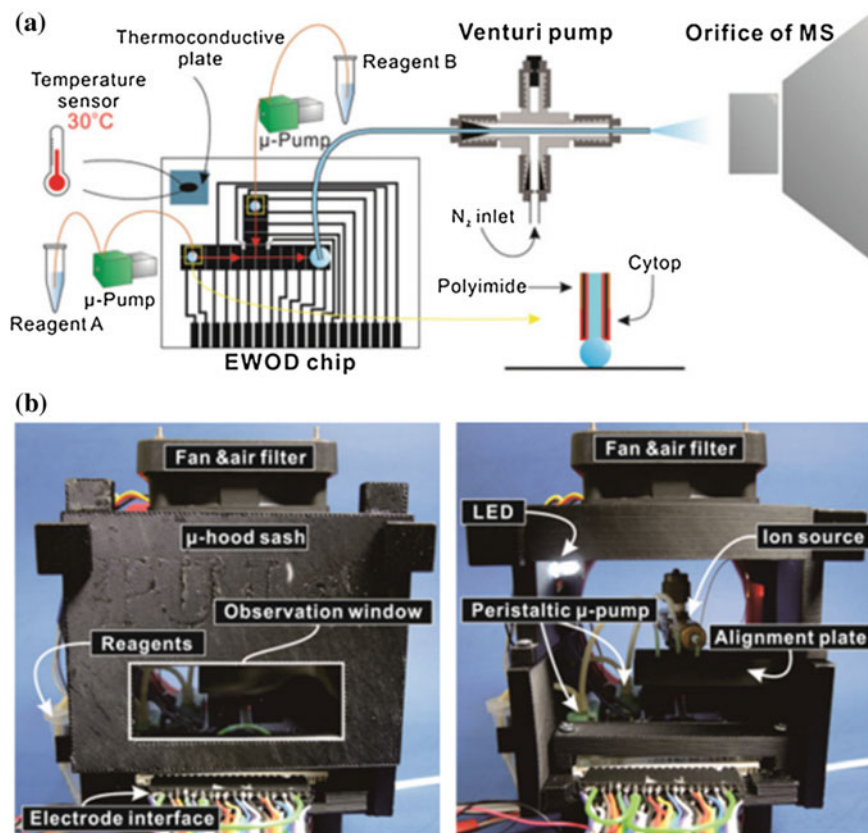


Fig. 6 A mass spectrometry system coupled with an open DMF device used for analytical analyses. Reproduced from [30] with permission from the Royal Society of Chemistry

coupling of a mass spectrometry system with a DMF device used for multiple analytical analyses [30].

2.2.3 Electrochemical Systems

Electrochemical detection is a sensing mechanism in which the change in an electrical signal (such as current, conductance, impedance, or potential) due to an enzymatic reaction on the sensing surface is measured [31]. The enzymatic reaction causes the chemical oxidation and reduction, which is associated with transfer of electrons, measured by the measurement equipment. Binding or the enzymatic reaction of the target analyte to the receptors immobilized on the sensing surface causes the change in the oxidation/reduction rate, which is used as a tool for

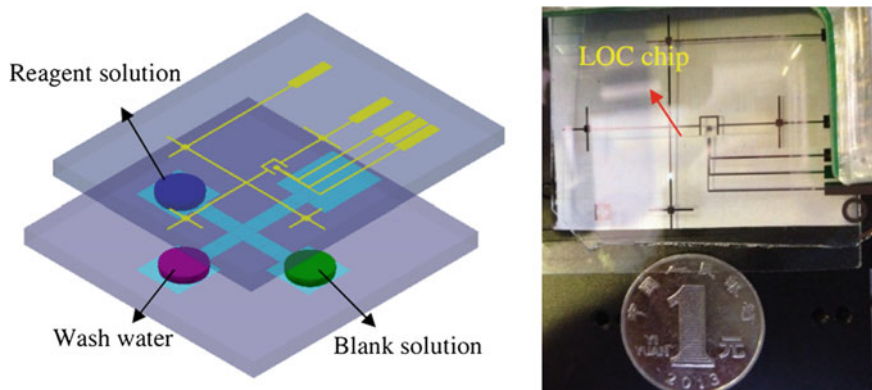


Fig. 7 Electrochemical biosensor integrated to a DMF platform for the analysis of ferrocenemethanol and dopamine. Reproduced from [33] with permission from IOP Publishing

detection [31]. These systems consist of three electrodes (the working, the auxiliary, and the reference electrodes) which are used for the measurement of the oxidation/reduction rates. These sensors are easy to fabricate, as they only require photolithographic patterning of the electrodes, making this method a widely used detection technique [20, 32]. Figure 7 shows an electrochemical biosensor integrated into a DMF device for the analysis of ferrocenemethanol and dopamine [33].

2.2.4 Other Systems

Optical, mass spectrometry, and electrochemical detection systems are the dominant mechanisms used for biochemical sensing on DMF devices. However, there are some other detection systems integrated into DMF devices which are usually electrical based. A field-effect transistor based biosensor has also been integrated into DMF systems for the detection of avian influenza virus [34]. These sensors are highly sensitive and function based on the change in the conductance of the semiconductor transducer due to the electric field around the biomolecules bound to their surface. Capacitive electrodes have also been used as transducers for biosensing purposes [35]. Other than these mechanisms, hydrodynamic manipulation of microbeads has also been used as a mean for the indication of the presence of low concentrations of DNA in liquid samples [36]: the presence of DNA in the sample changes viscoelasticity of the liquid which consequently changes the pattern of microbeads motion due to their hydrodynamic manipulation.

Regardless of the transduction mechanism used for biosensing and biochemical detection, biosensors are required to have high selectivity towards certain analytes in order to accurately detect them. The selectivity of the biosensors to a certain analyte is achieved by surface modifications. Different methods have been used for

the modification of the sensing surface of the biosensors [1] and based on these methods, the biosensors can be categorized as antibody-based [34, 35], enzyme-based [37, 38] and aptamer-based [39–41] systems.

3 Advances in Digital Microfluidics (DMF)

This section explains the new developments and advances made in digital microfluidic (DMF) devices with regards to biochemical applications. The advances in the fabrication of the devices is explained first. Then fluid manipulation techniques and advanced operators developed for assay processes are discussed.

3.1 Device Fabrication

Within the past two decades, several enhancements have been made in the fabrication procedures and material selection for the DMF devices to increase durability and resolution, and decrease the cost of the devices. Here we explain the individual components forming the DMF devices separately.

3.1.1 Substrate

Depending on whether the resolution, cost, or throughput of the device is the main criterion, the substrate used for DMF chips may be different. Normally, for in-laboratory and proof-of-concept experiments glass substrates are used due to the availability and versatility of the microscope glass slides [42]. When the resolution of the chip is important, silicon wafers with a thermally grown oxide layer are used as the substrate as these wafers provide a very smooth surface, allowing for the fabrication of very small features [43, 44]. On the other hand, for the low cost and disposable chips paper substrates are used [45]. For high throughput and durable devices, printed circuit boards (PCB), allowing for the fabrication of a large number of electrodes [46], are used. PCB chips have also shown to be cost-effective and used for applications requiring disposable chips [47].

3.1.2 Electrodes

Electrodes are mostly fabricated using the photolithography technique using the thin metal layers deposited on the substrate. In such a method of fabrication, the material used as the electrode does not significantly affect the resolution of fabrication, and hence, multiple different materials have been used for this purpose (e.g., copper, silver, and carbon [42, 48]). However, for the smoothness of the surface,

and avoiding the oxidation of the metal layer gold is the most widely used material [1]. One issue in the deposition of gold is its low adhesion to the substrates. In order to solve this issue, an adhesion layer such as a few nanometers of chromium or titanium is deposited first, and the gold layer is deposited on the top of this adhesion layer [21, 44]. In some applications, it is required to have optical access to the buffers on the chip for sensing purposes. For these cases, normally a transparent material such as indium-tin oxide (ITO) is used for the fabrication of electrodes [49]. The electrodes in disposable and flexible chips are fabricated using simpler methods such as screen or inkjet printing [50].

3.1.3 Insulating Layer

As explained in the Sect. 2.1.1, the insulating layer which separates the electrodes and the liquid (neglecting the hydrophobic layer), plays an important role in EWOD actuation as it prevents electrolysis of the liquid and allowing the application of higher voltages for manipulating the droplets. This layer has to be very uniform and free of pinholes to avoid the bridging of the electrical charges from the electrode to the liquid and the resultant electrolysis. Since the EWOD phenomena is a capacitive-based phenomenon, its magnitude is dependent to the dielectric constant and the thickness of the insulating layer, i.e., for higher dielectric constants and smaller thicknesses the EWOD effect is more significant [14, 51]. Figure 8 shows the contact angle of water as a function of the magnitude of the applied voltage in an EWOD setting with three different insulating layers of $(\text{Ba}_{0.7}\text{Sr}_{0.3})\text{TiO}_3$ (BST, $\epsilon \approx 180$), silicon dioxide (SiO_2 , $\epsilon \approx 3.7$) and a fluoropolymer ($\epsilon \approx 2 - 3$) [51]. The thicknesses of the three layers are 70 nm, 100 nm, and 120 nm, respectively. It could be observed that the change in the contact angle as a result of the applied voltage is significantly higher for BST than the other two materials. This is due to the higher dielectric constant and smaller thickness of BST as compared to the other layers.

Fig. 8 Variation of the contact angle of water versus the applied voltage for three different materials as BST (70 nm), silicon dioxide (100 nm), and a fluoropolymer (120 nm). Reproduced from [51] with permission from AIP Publishing

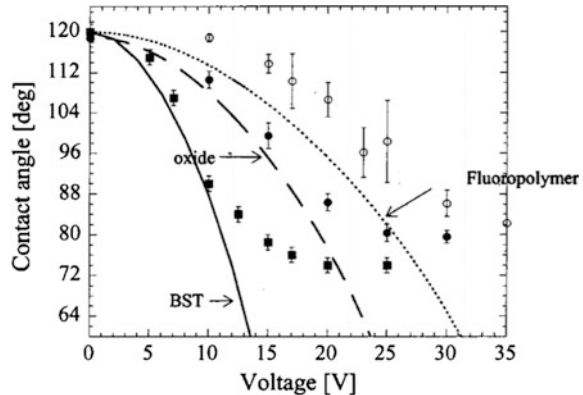
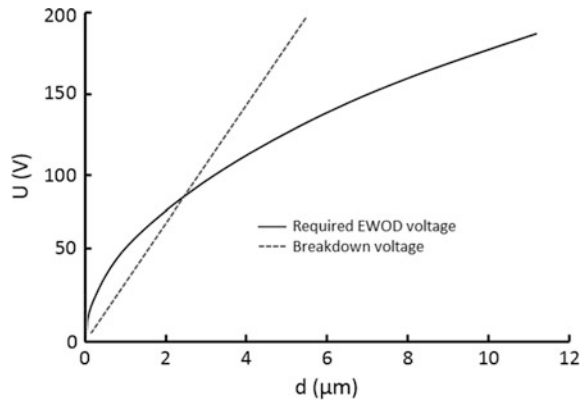


Fig. 9 Required electrowetting voltage (solid line) and the breakdown voltage (dashed line) versus the thickness of the insulating layer. The data belongs to water on a dielectric material with $\epsilon = 2$ [14]



Similarly, the change in the contact angle for the SiO_2 layer is larger than that of the fluoropolymer layer.

Smaller thicknesses of the dielectric layer result in stronger EWOD effect for a constant applied voltage. However, for each material, there is a limit smaller than which breakdown of the insulating layer occurs upon applying high voltages. Figure 9 illustrates two curves, one representing the required electrowetting voltage for droplet movement, and the other showing the breakdown voltage versus the thickness of the dielectric layer (material with $\epsilon = 2$) [14]. For this particular case, the two curves meet at the dielectric thickness of slightly higher than $2 \mu\text{m}$. Below this value, the electrowetting voltage is higher, meaning that before the droplet moves the insulating layer breaks down. For larger thicknesses, the electrowetting voltage is smaller, and therefore, the droplet can be moved without dielectric breakdown.

For the fabrication of DMF devices a variety of materials have been used as the insulating layer. Silicon dioxide [52], parylene C [10], and polytetrafluoroethylene (PTFE) have been widely used due to their availability. Photoresists such as SU-8 [53] and S1813 [42] have also been used as the dielectric layer due to their ease of deposition. However, the photoresists have poor dielectric properties. Finally, materials with high dielectric constants (such as BST [51] and Ta_2O_5 [54]) have also been used to reduce the required voltage for droplet actuation [1].

3.1.4 Hydrophobic Layer

Hydrophobicity of the chip surfaces is crucial for the transport of liquid droplets on the DMF chips. For this purpose, low surface energy materials must be used as the hydrophobic layer. Fluoropolymer materials such as Teflon [52] and Cytop [43] have been widely used as the hydrophobic layer for DMF devices.

3.2 Fluid Manipulation Techniques

The basic fluidic operations explained in Sect. 2.1.4 are the basis of sample manipulation on DMF devices [52]. This section focuses on the advances made towards enhancing the precision and speed of these operations.

3.2.1 Droplet Transport

Droplets are transported on DMF devices by sequentially actuating the electrodes. To enhance the speed of transport, several attempts have been made including modulation of the applied voltage and using different surrounding media [14]. In early studies, DC voltages were used for droplet actuation. It was shown that applying AC voltages enhances sample manipulation and increases the chip lifetime [14]. Later on, it was shown that applying pulses of DC voltage rather than normal AC or DC voltages will further improve the chip lifetime and speed of transport [55]. The use of silicone oil [53, 56] or mineral oil [57] instead of air as the surrounding media also reduces the interfacial tension and contact angle hysteresis, enhancing the droplet motion. These oils were shown to be bio-compatible [57]. Figure 10 shows the transport of gelatin methacrylate hydrogel (GelMA) and growth media in mineral oil for cell patterning applications [57]. Hydrogels such as

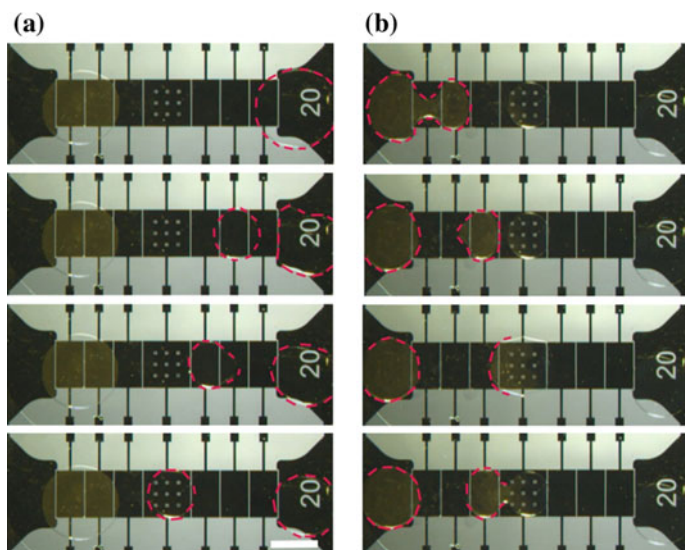


Fig. 10 Transporting gelatin methacrylate hydrogel (GelMA) and growth media in mineral oil for cell patterning applications. Reproduced from [57] with permission from the Royal Society of Chemistry

GelMA are highly viscous and sticky and cannot be transported on the chip when the surrounding media is air.

3.2.2 Droplet Splitting and Dispensing

The splitting and dispensing operations were explained in Sect. 2.1.4. Splitting is performed on an array of three electrodes by simultaneous actuation of the two side electrodes which results in pinching off and splitting the mother droplet into two daughter droplets. Dispensing from a reservoir droplet is also performed by actuating the reservoir electrode and the second adjacent electrode to the reservoir. This procedure without controlling the magnitude of the applied voltage will result in a deviation of 5% or higher in the volume of the split/dispensed droplets [58]. Several strategies have been proposed to enhance the accuracy of splitting and dispensing. For instance, the capacitance of the droplet is used as a mean to determine its volume. In this approach, a feedback control system is used to modulate the applied voltages to the two side electrodes [58] to accurately control the droplet volume. This strategy has improved the precision and reduced the deviation in the volume to 1%. In another study, to improve the precision of droplet dispensing, the middle electrode was turned on at the same time as the two side electrodes, and then the voltage applied to the middle electrode was ramped down until the droplet split [59]. Samiei et al. [42] showed that precise droplet splitting with an error less than 1% can be achieved using an applied voltage close to the threshold value for splitting. This method does not require any feedback control or voltage modulation system. Also, once the physical properties of the chip are determined this method is very easy to implement. They showed that the threshold splitting voltage is a function of the gap height when other parameters are kept the same. The relationship between the threshold voltage versus the gap height has been determined and these results are shown in Fig. 11 for three different electrode geometries. This

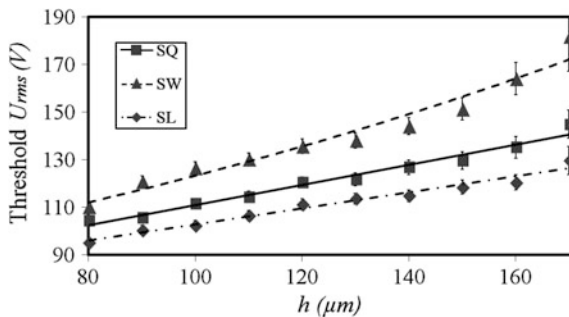


Fig. 11 Threshold voltage required for droplet splitting versus the gap height between the top and the bottom plates for three different electrode geometries as SQ (square), SW (stripped along the width of the electrode) and SL (stripped along the length of the electrode). Reproduced from [42] with permissions from IOP Publishing

figure shows that for a wide range of the gap height, this relationship is linear which facilitates the selection of a proper voltage based on the chosen gap height.

3.2.3 Droplet Mixing

It was explained that the basic mixing method on DMF devices is based on transporting the droplet over an array of three or four electrodes. However, this method is very inefficient and results in a relatively long mixing process. Later on, different 2D arrays of electrodes were studied for mixing and it was found that cyclic transport of the droplet over a 2×4 array of electrodes provides the best mixing performance [60]. This method also includes cyclic transport of the droplet over the chip surface which occupies a portion of the chip. The major problem with this method is that upon the presence of biological species (which have the tendency to adsorb to the surface) this method can increase the chance of chip breakdown. Most recently, an electrohydrodynamic (EHD) technique was implemented for rapid droplet mixing while the droplet is stationary [61]. The mixing using this method could be performed within less than 1 s, and the method was tested for different buffers including deionized water, phosphate-buffered saline (PBS), and sample containing DNA. The technique can be performed using the actuating electrodes on DMF devices and works for both open and closed systems. Figure 12 illustrates the EHD mixing method for different samples of polystyrene microbeads and safranin-o dye on both open and closed DMF devices.

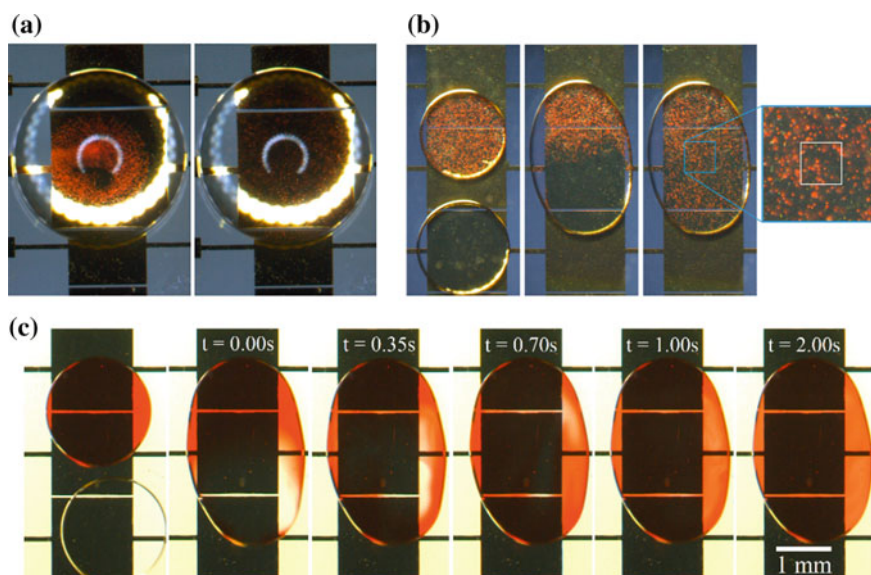


Fig. 12 Electrohydrodynamic mixing of **a** sample containing polystyrene microbeads (PS) on an open system DMF chip, **b** sample containing PS on a closed system DMF device, and **c** sample of safranin-o dye and DI water on a closed system DMF device. Reproduced from [61] with permission from the Royal Society of Chemistry

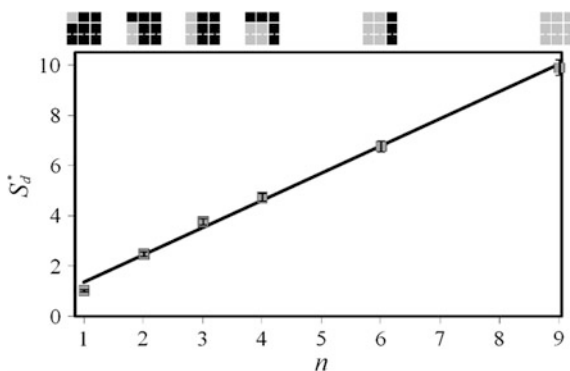
3.3 Advanced Operators

While the basic fluidic operations can be used for the manipulation of liquid samples, the entire sample preparation processes may not be feasible only using these operations. Some applications require variable volumes of different samples to be generated. In some applications which include microbeads, one needs to concentrate them within the droplet. In cell-based applications, patterning of the cells might be required. Also, heating is a part of multiple applications. For these purposes, specific strategies have to be adopted to perform the process. Here the techniques that have been developed for such processes are discussed briefly.

Droplet dispensing using the conventional method can produce constant volumes of droplets proportional to the size of the electrode. Therefore, if one needs to mix two samples with different volumes, either one of the samples has to have a large volume (and resultant contact area) which is difficult, if not impossible, to manipulate on the chip, or several dilution steps have to be used to reach the desired ratio of the samples in the mixed droplet. One way to avoid this issue is to have the ability to dispense variable volumes of liquid on the chip. The first strategy developed for dispensing variable volumes of droplets is based on applying different voltages to the reservoir and the dispensing electrode [58]. This study used capacitive sensing for determining the droplet size and a feedback control system to modulate the voltages applied to the reservoir and the splitting electrode. Lower voltages applied to the splitting electrode resulted in a lower size of the dispensed droplet. A different strategy, which was recently developed, is based on the geometrical modification of one of the electrodes by dividing it into several sub-electrodes [42]. It was shown that applying the threshold splitting voltage results in high-precision droplet dispensing. Also, it has been shown that the size of the droplet (measured based on its normalized area) has a linear relationship with the number of the sub-electrodes (Fig. 13), allowing for choosing the proper number of sub-electrodes based on the desired volume of the droplet.

Microbeads are used in several immunoassays for capturing the target analytes and labeling them for fluorescent microscopy [62]. Typically, magnetic microbeads

Fig. 13 The normalized area of the dispensed droplet versus the number of actuated sub-electrodes. Reprinted from [42] with permission from IOP Publishing



are used for this purpose where the functionalized beads are mixed in the sample to capture the target analyte which are then collected using an external magnet [63]. Recently, some techniques have been developed to eliminate the need for an external magnet for concentrating the beads inside the droplet. In a recent study, it has been shown that rotation of the droplet containing beads can focus the beads in one area. For this purpose, the chip includes a central electrode surrounded by several electrodes. One end of the droplet is fixed by continuous actuation of the central electrode, while the rest of the droplet spins around the central part by sequential actuation of the surrounding electrodes [36]. This rotational motion of the droplet causes the collection the beads in the center of the droplet due to the hydrodynamic-density based phenomenon. After collecting the beads, the droplet was then split to keep one side highly concentrated and the other side with a small concentration of the beads. In a different study, a dielectrophoretic-gravity driven (DGD) technique was developed for concentrating the microbeads [64]. By combining the effects of negative dielectrophoresis and gravity, the beads were collected in the center of one electrode. Then, the droplet was split into two parts one with majority of the beads and the other with a small concentration of the beads. The advantage of DGD technique is that it can be performed using the conventional electrodes and on any location of the chip. An example of the DGD method is shown in Fig. 14. The combination of the DGD technique and the methods proposed for dispensing variable volumes [42] of droplets can be a powerful method for pre-concentration of the samples for immunoassays.

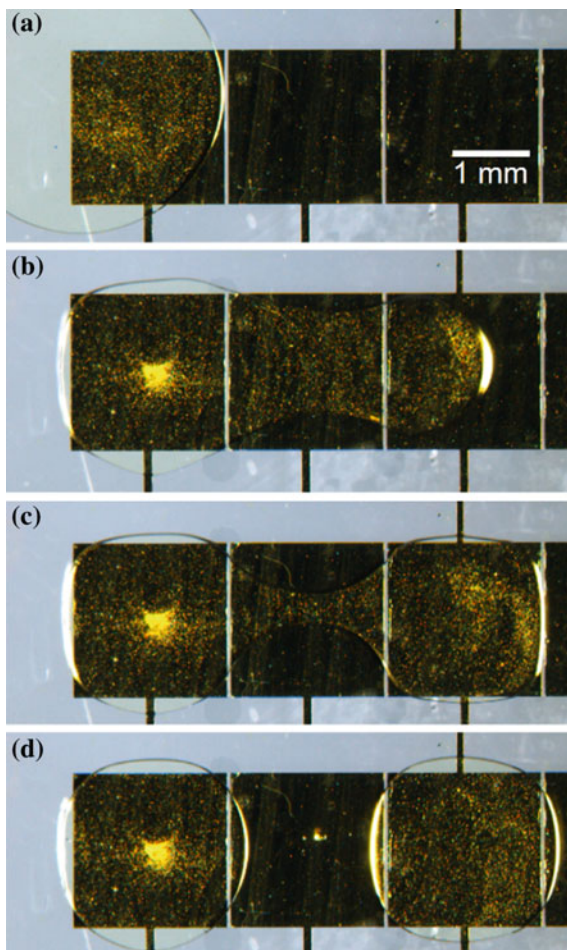
Microheaters have also been integrated to the DMF devices for the applications requiring the control on the temperature of the assay [25, 65]. The heaters were either external modules added to the chip [25] or were fabricated on the chip using the similar fabrication method used for patterning the actuating electrodes [65].

3.4 Anti-biofouling Techniques

The hydrophobic layer on the DMF chips facilitates the motion of the droplets for both aqueous and non-aqueous buffers and prevents cross contamination. However, some biological species such as proteins and lipids have the tendency to stick to the surface through the hydrophobic adsorption or electrostatic interaction [1]. The biomolecular adsorption hinders the manipulation of liquid samples and increases the chance of cross contamination. The strategies used for preventing biofouling in conventional biological equipment [66] (test tubes) or continuous microfluidic devices [67] may not be practical for DMF chips as the addition of any coating may reduce hydrophobicity as well as the effect of EWOD. Thus, approaches specifically developed for preventing biofouling in DMF devices are discussed here.

The primary strategy used for reducing the tendency of the proteins to the surface is through controlling the pH of the buffer and modulating the applied voltage to the electrodes [68]. This technique reduces the biofouling effect, however, the permanent effects on the surface have been observed. The use of silicone

Fig. 14 The sequences of images from the concentration of silica beads using DGD technique. Reproduced from [64] with permission from AIP Publishing



oil as the surrounding media is another strategy which is very effective, preventing biofouling even for the whole blood for thousands of cycles of transport on the chip [22]. However, using oil might limit applications such as those with integrated biosensors on the chip surface. The use of silicone oil as a thin shell around the droplet rather than the entire surrounding media has also been proposed for anti-biofouling purposes [56]. In this method, before pipetting the samples in the reservoirs, the chip surface is touched with a pipette tip initially immersed in oil. This leaves a $\sim 0.1 \mu\text{L}$ oil droplet on the surface. When the sample droplet is placed on the reservoir, the oil spontaneously forms a thin layer around the entire droplet [53]. A similar strategy was proposed using Pluronic F127, which functions as a surfactant, forming a shell around the droplet to prevent biofouling [69]. Using Pluronic F127, samples containing up to 1 mg/mL proteins have been manipulated on the chip with negligible surface contamination, proved through confocal

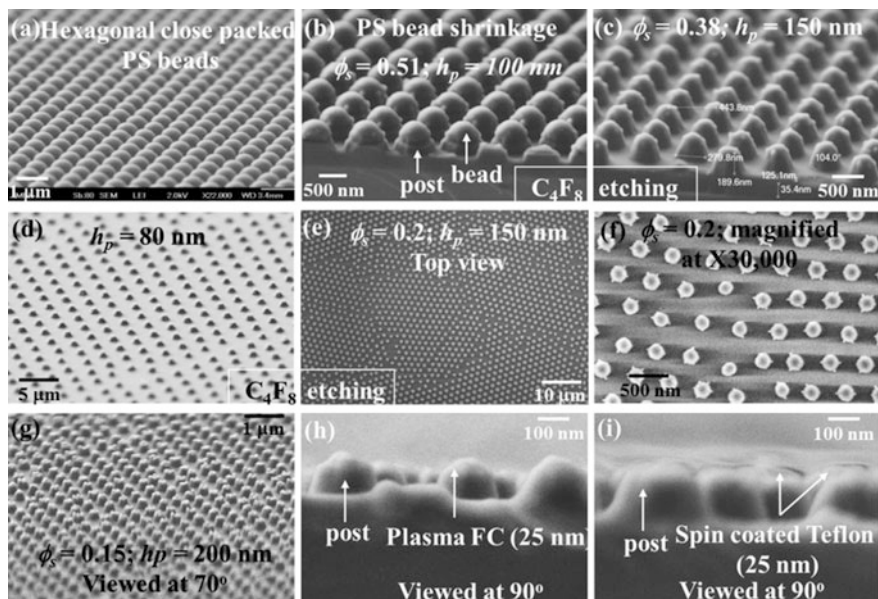


Fig. 15 Samples of different nano-structures made on the surface to create a superhydrophobic and anti-biofouling surface. Reprinted from [72] with permission from Elsevier

microscopy and mass spectrometry. A different method, simple but effective, has been the use of disposable polymer “skins” as the hydrophobic layer [70]. The polymer skins can significantly reduce the protein adsorption, and for every round of experiments, a new skin can be applied to the chip, allowing for reusability of the chip. Generation of a nanostructured superhydrophobic layer by the aid of methods such as plasma deposition of fluoropolymers is another technique to significantly reduce biofouling on the chip surfaces [71, 72]. Figure 15 shows different nano-structures for generating superhydrophobic surfaces and enhancing anti-biofouling effects [72].

4 Digital Microfluidic (DMF) Platforms for Biochemical Sensing Applications

In the previous sections, digital microfluidics (DMF) along with the biochemical sensing mechanisms integrated to or paired with DMF were introduced, and the advancements made in DMF for lab-on-a-chip (LOC) applications (specifically for biochemical detection purposes) were discussed. This section includes the applications of DMF platforms involving biochemical sensing processes.

As explained in Sect. 2.2, detection on DMF devices can be categorized into off-line and on-line modes. This classification is based on whether the detection is performed off the chip (off-line) or using a detection system integrated into the chip and as a part of the on-chip processes (on-line) [1, 20]. The off-line detection mode has widely been used since the introduction of DMF, as the equipment used for biochemical sensing such as microscopy and mass spectrometry devices) already existed in laboratories while DMF has been used for sample preparation, partially or entirely [1]. On the other hand, the tendency towards developing microfluidic packages for performing the entire assay processes, including biochemical sensing on the chip, has resulted in the miniaturization and integration of sensing techniques into the chip for on-line detection. Here we go over the implementation of DMF devices for applications involving biochemical sensing.

4.1 Off-Line Mode

As discussed earlier, in off-line detection modes either the sample or the chip with the sample therein is taken to the detection equipment, which is mostly a microscope or mass spectrometer [1]. While other sensing mechanisms might have also been used for off-line detection, here the optical and mass spectrometry mechanisms are discussed due to their popularity.

4.1.1 Optical Detection

Optical systems are probably the most widely used systems for off-line detection on DMF [73]. Optical systems are categorized into fluorescence, absorbance, chemiluminescence, and surface plasmon resonance (SPR) systems which were explained in Sect. 2.2.1.

Several studies have used fluorescence microscopy as the sensing mechanism for performing biochemical assays on DMF [74]. For instance, one study has shown the possibility of performing polymerase chain reactions (PCR) on DMF [75], in which the sample transport and mixing was performed by EWOD actuation of the sample droplets. To perform the amplification of the DNA sequences, a PCR chamber was created on the chip using the hydrophilic/hydrophilic surface and generating surface tension gradient. Microheaters and temperature control units were also integrated into the chip to control the reactions. The platform was used for the amplification and detection of Dengue II gene. Fluorescent microscopy was used for the detection of the amplified samples and their results showed significantly reduced amount of the consumed buffers and the operation time of the assay using the DMF platform in comparison with the macro-scale counterpart. Another study has shown the application of DMF for proteolytic digestion assays [70]. In this study, an open DMF system was used with the removable skins as the dielectric and hydrophilic layer. The dried spots of the digestive enzymes were formed on the

chip surface. These so called “skin depots” were used for the protein digestion assay. Fluorescence measurements were performed for the evaluation of the shelf life of these skin depots when stored at $-80\text{ }^{\circ}\text{C}$. The results showed that the activity of the dried enzymes can be retained with a high performance over a period of one month. Single cell analysis using DMF was shown in [76] in which a parallel plate DMF device was used for the manipulation of the cell droplets and isolating single cells, followed by cytotoxicity analysis. An array of hydrophilic microwells was formed on the chip surface where after transporting the droplet over the array, single yeast cells (*Saccharomyces cerevisiae*) were isolated. The effect of Amphotericin B agent was studied on the membrane integrity of the isolated cells by transporting the droplet of the agent over the array of isolated cells. This effect was monitored using time-lapse fluorescence microscopy. Figure 16 illustrates the schematic of the sample preparation, on-chip assay processes, and fluorescence microscopy for this cytotoxicity analysis.

The application of DMF coupled with off-line absorbance and chemiluminescence measurement techniques is shown for a magnetic bead based heterogeneous immunoassay on human insulin and interleukin-6 (IL-6) [77]. The steps required for the immunoassay including concentrating beads, washing steps, bead retention, and resuspension of beads were performed using a parallel plate DMF device. The collection of the magnetic beads and washing steps were carried out by the aid of an external permanent magnet. The efficiency of the washing protocol was monitored and optimized by absorbance measurement using a plate reader. Based on an 8 min enzymatic reaction and the results of the traditional washing method, it was found that five cycles of washing process are required to achieve similar absorbance signals. Chemiluminescence detection was carried out for detection of antibody binding using a photo-multiplier tube and a multi-well-plate reader, and the kinetic curves were formed for both insulin and IL-6.

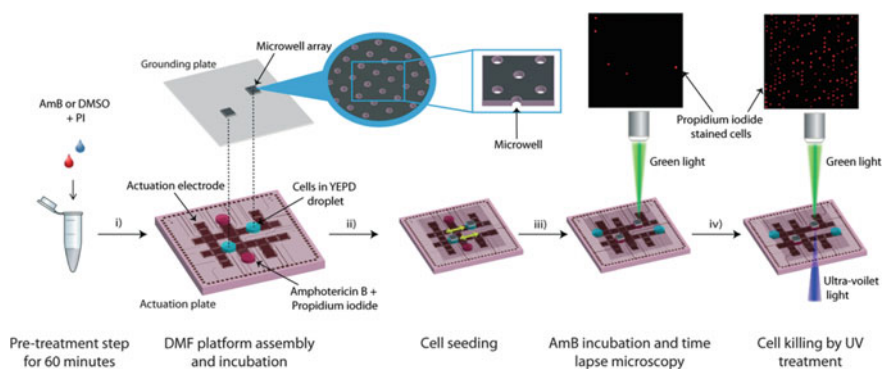


Fig. 16 Schematic of the sample preparation, on-chip assay processes, and fluorescence microscopy for the cytotoxicity analysis the yeast cells. Reproduced from [76] with permission from the Royal Society of Chemistry

4.1.2 Mass Spectrometry

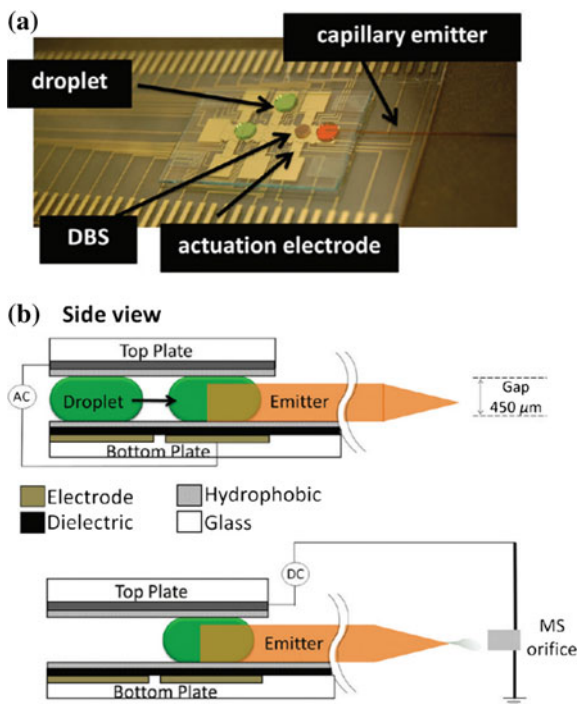
As explained earlier, mass spectrometry is based on sorting the chemical species within the sample into a spectrum which depends on the mass-to-charge ratio of the species. This is carried out by ionizing the sample which results in the breakdown of the sample molecules into charged fragments. By passing these ions through an electric or magnetic field, the spectrum of the species within the sample is formed and the content is identified. Therefore, this method is used as an off-line method by coupling a bulky device with the DMF chip and transferring the sample from the chip to the spectrometer [78]. The study on proteolytic digestion assays, which was discussed earlier for fluorescence analysis of the shelf life of the dried enzyme spots, used mass spectrometry for the measurement of the enzymatic reaction products [70]. After sample preparation conducted by mixing several buffers and reagents, the final product was transported to the dried spot and incubated until the reaction was completed. Then, the sample was allowed to dry and finally the skin was peeled off of the device and processed using mass spectrometry.

Coupling the DMF sample processing unit with mass spectrometry has also been shown for the analysis of dried blood spots (DBS) from newborns [79]. The coupled platform is used for the study of succinylacetone (SA), which is a biomarker for hepatorenal tyrosinemia. The quantification of SA in DBS samples is performed using a nanoelectrospray ionization mass spectrometry (nESI-MS). The sample preparation is performed by actuating the droplets of buffers and reagents on the DBS. A glass capillary emitter which is sandwiched between the bottom and top plates of the DMF device is used for transferring the products from the DMF chip to nESI-MS device. Figure 17 shows the DMF device and the capillary emitter, as well as the schematic of the nESI-MS system coupled with the DMF device for the SA quantification assay.

4.2 *On-Line Mode*

Introduction of microfluidics (such as DMF systems) has been based on the desire to downscale biochemical assays, automate the processes, and develop point-of-care devices for the diagnosis purposes. As part of this miniaturization step, detection systems have been downscaled and integrated into the DMF devices to allow for the on-line detection of target analytes. Several challenges have been associated with the integration of these detection systems into DMF. These challenges are related to the geometrical configuration and the method of sample manipulation on the DMF devices. This section reports different detection technologies integrated into DMF devices for on-line detection purposes.

Fig. 17 a DMF device and the capillary emitter, and b the schematic of the nanoelectrospray ionization mass spectrometry system coupled with the DMF device for the analysis of DBS from newborns. Reproduced from [79] with permission from ACS Publications



4.2.1 Integrated Optical Detection Systems

Originally, the optical detection techniques were operated using bulky devices such as microscopes and plate readers. Development of miniaturized exciters and photodetectors has enabled the integration of the optical detection systems into microfluidic devices. In DMF devices, the integration of the majority of the optical-based detection systems requires at least one of the two plates to be transparent, which is achieved using ITO as the electrode [1].

On-line fluorescence detection has been shown for the magnetic bead based assays on a DMF platform [80]. The DMF device has been fabricated using a PCB which allows for easy assembly of the device. A magnet is used for collecting the beads for washing steps. A Peltie element and a thermal sensor were integrated into the chip for temperature control. The fluorescence detection is carried out using a CCD camera and two lasers, assembled to the device. The DMF platform and the integrated CCD is shown in Fig. 18. Another study shows the application of DMF with an integrated fluorescence measurement system for the enzymatic detection of r Fabry, Pompe, Gaucher, Hunter, and Hurler diseases [47]. Disposable cartridges were used as DMF chips, and the fluorometric enzymatic assay was performed on newborn DBS punches on the cartridge. Lysosomal enzymatic activities were

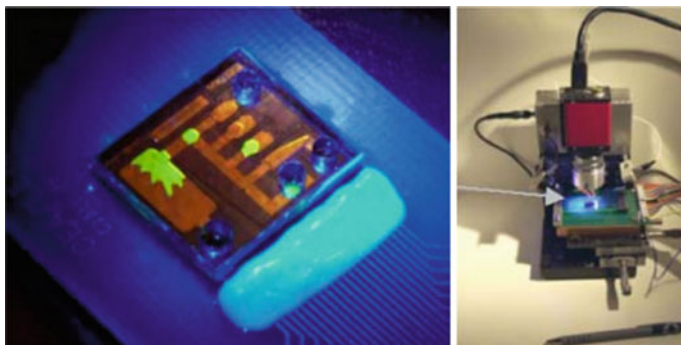


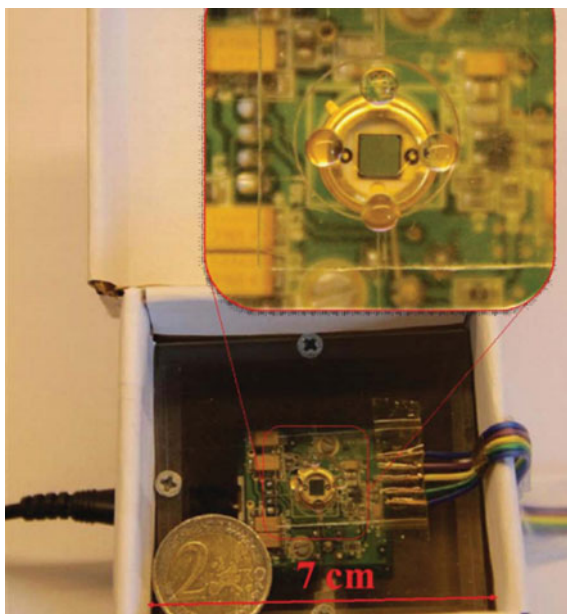
Fig. 18 The DMF device and the assembled CCD camera for an on-chip fluorescence measurement. Reproduced from [80] with permission from Springer

measured using the integrated fluorescence detection system. More than 98% linearity was shown for their range of measurements. In a different study, complementary-metal-oxide semiconductor (CMOS) integrated circuit was used for quantitative-polymerase-chain-reaction (qPCR) analyses with all required components integrated into the platform [23]. Temperature was controlled by the aid of resistive aluminum temperature sensors and polysilicon heaters. Geiger-mode single-photon avalanche diodes were integrated into the platform for the measurement of the fluorescence intensity. High voltage required for droplet actuation was also generated using an integrated circuit on the chip. Detection of *Staphylococcus aureus* was performed as a proof of concept. The integrated platform showed reliable and sensitive analysis of qPCR.

Integration of absorbance-based optical detection systems into DMF has been shown in multiple studies for online detection [21, 22]. Such a platform has been used for a colorimetric enzymatic glucose assay which was used for the analysis of body fluids (plasma, serum, urine, and saliva) [22]. The detection system consisted of an LED light source installed underneath the bottom plate, and a photodiode on the top plate to measure the intensity of the incident light. Thus, both bottom and top plates were fabricated using transparent electrodes (ITO) to allow for the optical connection between the light source and the detector.

Application of the on-line chemiluminescence detectors on DMF devices has been shown in several studies [49, 81, 82]. A portable compact DMF-based platform was developed with an open DMF system as the sample handling unit and a chemiluminescence detector for the analyte detection. It has been shown that ball-like droplet shape in the open DMF system focuses the fluorescence and improves the sensitivity of detection. It was also shown that such an improvement increases by increasing the contact angle of the droplet. Using this method, a detection limit of 10 $\mu\text{mol/L}$ was found for H_2O_2 -luminol (3-aminophthalhydrazide)-HRP. Figure 19 shows this open system DMF device with the integrated chemiluminescence detector. In another

Fig. 19 An open DMF platform integrated with a chemiluminescence detector. Reproduced from [49] with permission from the Royal Society of Chemistry



study, electrochemiluminescence (ECL) detectors were integrated onto the top plate of a parallel plate DMF device for microRNA analysis [82]. The light generated by electrically excited luminophores in the droplets of tris(phenanthroline)ruthenium(II) and tripropylamine (TPA) solutions was detected by the ECL detector. The integrated system was used for an oligonucleotide hybridization assay in which single nucleotide mismatches were detected. A detection limit of 1.5 femtomoles was found for the system.

Surface plasmon resonance (SPR) is highly sensitive, and due to its small size, integrated into DMF devices for on-line detection [28, 83, 84]. An example of such integration is shown in Fig. 20, where the sensing surface of the SPR detector is patterned on the top plate and in contact with the liquid sample. The measurement is performed using a laser source and the CCD camera, which emits and detects the laser beam through a prism placed or assembled on the top of the top plate [83]. As a proof of concept, such a platform has been used for the detection of different concentrations of NaCl in ultra-pure water. The same setup was used for the detection of DNA hybridization [84], where both DNA probe immobilization and the subsequent hybridization reactions were detected, as the immobilized probe density was actively controlled. It has been shown that a twofold increase in the SPR signal (as compared to passive probe immobilization) is achievable when immobilization of the probes is actively controlled using negative electrical potential. Using this integrated platform, a detection limit of 500 pM of DNA was obtained. In another study, the same device was further enhanced by patterning a

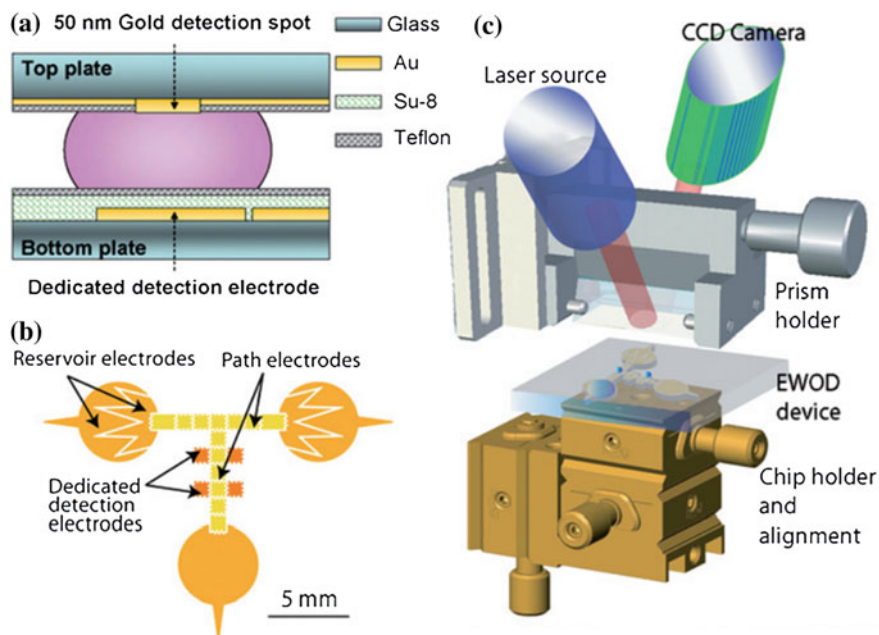


Fig. 20 Schematic of a DMF device integrated with a SPR detection system. **a** The components of the chip, **b** the design of the DMF platform, and **c** the assembly of the SPR with the DMF device. Reproduced from [83] with permission from the Royal Society of Chemistry

2D array of gold nanostructures. Colloidal-gold nanoparticles were used as the labels amplifying the SPR signal [28].

4.2.2 Integrated Electrochemical Detection Systems

Electrochemical detection systems are the most suitable detectors to be integrated into DMF platforms, as they can easily be patterned and functionalized on the top plate of the DMF devices [1, 20]. Several studies have shown successful applications of these devices for biochemical sensing on DMF platforms [33, 85, 86]. The study which was previously shown in Fig. 7 illustrates an example of such an integration, in which the bottom plate contains the actuating electrodes for sample manipulation and the electrochemical sensor, along with the DMF ground electrode, is located on the top plate [33]. Through a series of cyclic voltammetry, an analysis of ferrocenemethanol (FcM) and dopamine (DA) was performed, illustrating the high compatibility and ease of integration of such a detector. A linear calibration curve was obtained for DA for a wide range of concentrations. Also, a detection limit of 420 nM was obtained for this detection system.

Recently, a DMF platform including an electrochemical sensor has been developed for selective detection of thyroid stimulating hormone (TSH) biomarkers [85]. The top plate includes the ITO ground electrode, as well as the patterned gold working electrode and the silver counter and reference electrodes. This assay was a magnetic bead based assay in which the microbeads were functionalized with primary antibodies for capturing the TSH antigens. Through several incubation and washing steps, the sandwich format (primary antibody-TSH antigen-enzyme conjugated antibody) was formed on the beads. For the amperometric sensing the horseradish peroxidase enzymes (HRP) were used which in reaction with 3,3',5,5'-tetramethylbenzidine could generate proper oxidation-reduction. A limit of detection of 2.4 $\mu\text{IU/mL}$ was found for the this integrated system. In a different study, a similar configuration was used for the detection of rubella virus (RV) IgG; the electrodes were modified to have a nanostructured surface. It was shown that the nanostructure increases the sensitivity of the electrochemical sensing significantly. The limit of detection was reported as 0.07 $\mu\text{IU/mL}$, which is a very low concentration for the detection of RV IgG. The schematic of the DMF platform, the three electrochemical sensing electrodes, and the nanostructured surface of the sensing electrodes are shown in Fig. 21.

4.2.3 Other Integrated Systems

Although majority of the detection systems integrated into DMF devices are optical and electrochemical based, some studies have used other detection methods for biosensing on DMF devices. For instance, a digital microfluidic impedance sensing platform was developed for the detection of Interleukin-6 through an ELISA assay [87]. A detection limit of 50 pM was reported for the integrated system. Another study has shown the integration of a capacitive biosensor into a DMF platform for the detection of *Cryptosporidium* oocysts in water samples [35]. Samples with different concentrations of cells were tested, and a calibration curve was obtained for the detection system. Integration of field-effect-transistor based biosensors into DMF devices have also been shown for the detection of avian influenza antibodies [34]. This study is based on the integration of the biosensor within the actuating electrodes on an open DMF device, as shown in Fig. 22. Although the fabrication of the device is very complicated (involving multi-layer patterning of the electrodes, dielectric separators, and semi-conductive material) the developed device showed a very high sensitivity with a limit of detection of 6.67 fM.

4.3 Post-sensing Sample Removal

Integration of different types of biochemical detection systems into DMF devices was shown in the previous section. Significant improvements in detection of proteins and cells were shown by the combination of the DMF sample preparation unit

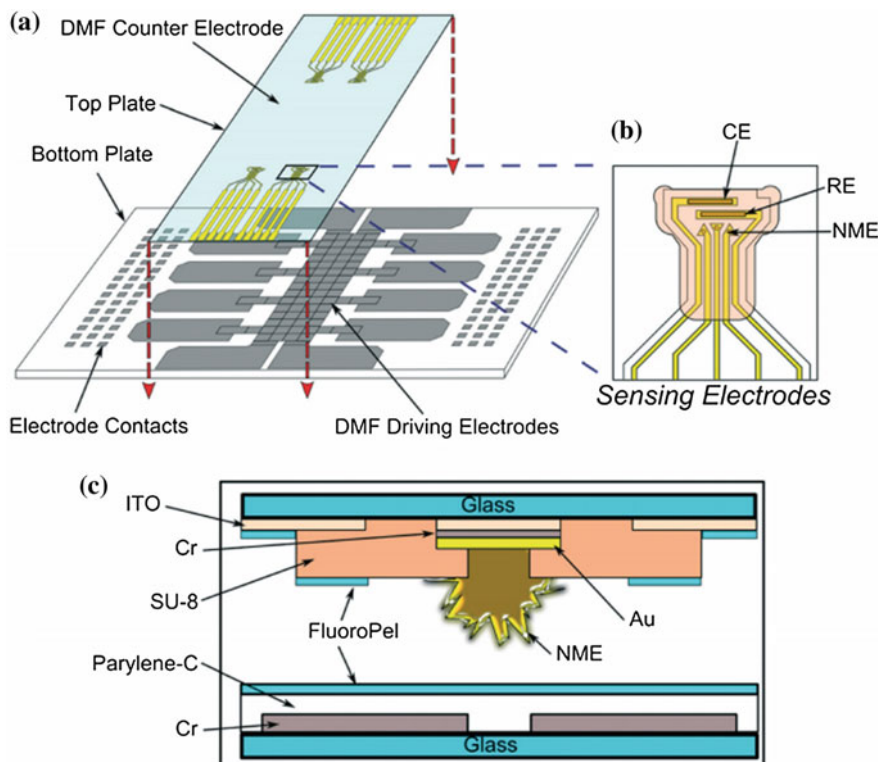


Fig. 21 The schematic of the DMF platform, the three electrochemical sensing electrodes, and the nano-structured surface of the sensing electrodes used for the detection of rubella virus IgG. Reproduced from [86] with permission from the Royal Society of Chemistry

and the integrated sensing system. However, one important issue is yet to be addressed, which is the complete removal of the sample from the sensing zone. Detection in many optical-based systems (e.g., fluorescence and absorbance) occurs through the liquid and such systems do not include a sensing surface. On the other hand, many other systems such as SPR, electrochemical, impedance, and FET systems include a sensing surface which consists of the transducer surface, and the immobilized receptors in many cases. The sensing surfaces are exposed to the sample through a window in which the hydrophobic layer is removed. In the case of the detection systems without the immobilized receptors, such as electrochemical systems, the sensor can be reused multiple times. The reusability of the systems with immobilized receptors is limited to biochemical regeneration of the sensing surface. However, incubation of the target analyte, washing cycles and sensing might require multiple steps of transportation of the buffer to and removing from the detector. The sensing surfaces have hydrophilic properties which hinder the transport of droplets on the DMF devices [35]. Therefore, if the sensing surface is

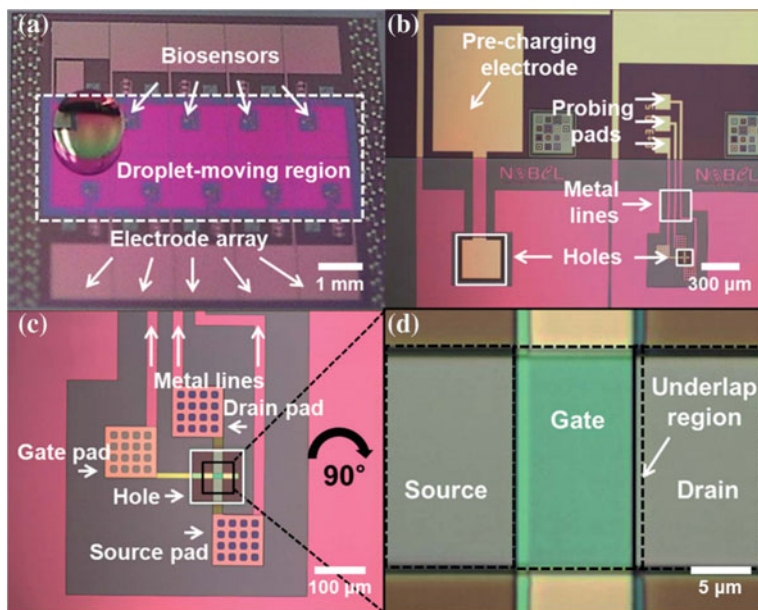


Fig. 22 An open DMF device with integrated FET biosensors for the detection of avian influenza antibodies. Reproduced from [34] with permission from the Royal Society of Chemistry

not designed properly or its surface area is too large, the droplet cannot be removed from the sensing unit after the detection process. In some studies the sensing window is designed very small to allow for the removal of the droplet [33, 84]. Although these studies have shown successful detection with the designed sensing area, it is desired to find the largest possible sensing area for the detection system without the limitation on droplet removal. A systematic study performed in [35] shows the optimized configuration and dimension of the rectangular hydrophilic and super-hydrophilic surfaces (HS) sensing area on which EWOD-based droplet removal from the detector is feasible. In this work, the minimum required voltage for removal of the droplet was studied for different surface wettability conditions, aspect ratios of the HS, and gap height of the parallel plate DMF device. Figure 23a shows examples of successful droplet removal from a gold HS surface. This study suggests the smaller the HS and the higher the aspect ratios (longer and lower width) the smaller the required applied voltage for droplet removal (Fig. 23b). Also, it has been shown that for super-hydrophilic surfaces, if the gap height is less than a certain threshold (e.g., 11% of the length of the electrode), the droplet will split on the HS, hindering complete droplet removal. They reported successful droplet removal from super-hydrophilic HS (e.g., gold with immobilized antibodies) as large as 13.3% and normal hydrophilic surfaces (e.g., sputtered gold) over 22% of the area of the actuating electrodes.

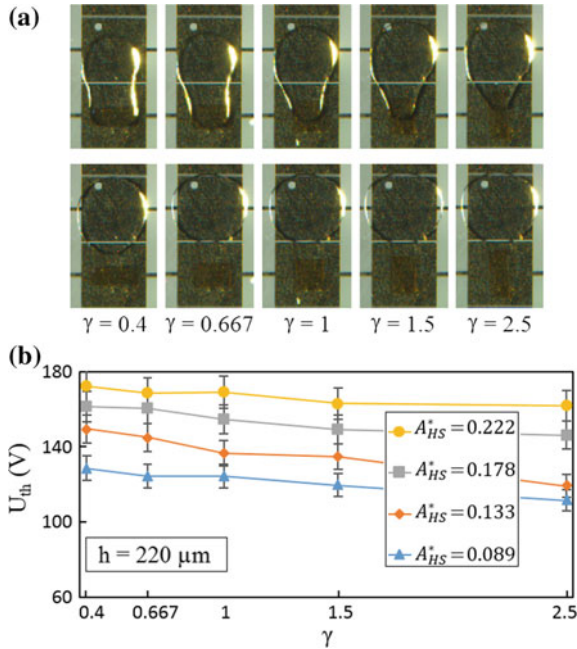


Fig. 23 a EWOD droplet removal from gold HS with different aspect ratios, and b the minimum required voltage for droplet removal for different sizes and aspect ratios of HS. Reproduced from [35] with permission from Elsevier

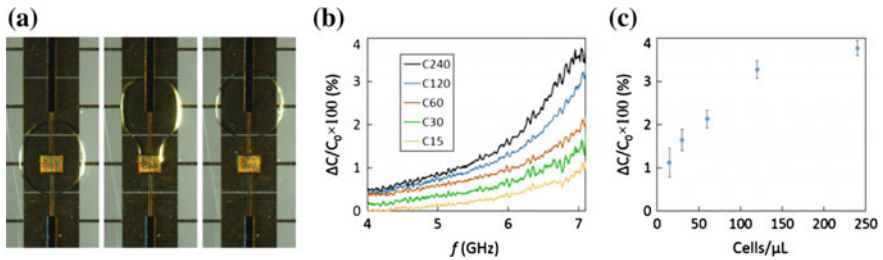


Fig. 24 A capacitive biosensor integrated into a DMF platform for the detection of different concentrations of *Cryptosporidium* oocysts. Reproduced from [35] with permission from Elsevier

Based on the optimum geometry found in the above study [35], a capacitive biosensor was developed and integrated into a DMF platform for detecting different concentrations of *Cryptosporidium* (as explained in the previous section). Such a configuration allowed for the detection of *Cryptosporidium* and complete droplet removal, as shown in Fig. 24.

References

1. Samiei E, Tabrizian M, Hoorfar M (2016) A review of digital microfluidics as portable platforms for lab-on-a-chip applications. *Lab Chip* 16(13):2376–2396
2. J. Z. Chen, S. M. Troian, A. A. Darhuber, and S. Wagner, “Effect of contact angle hysteresis on thermocapillary droplet actuation,” *J. Appl. Phys.*, vol. 97, no. 1, 2005
3. Darhuber AA, Valentino JP, Troian SM, Wagner S (2003) Thermocapillary actuation of droplets on chemically patterned surfaces by programmable microheater arrays. *J. Microelectromechanical Syst.* 12(6):873–879
4. Lehmann U, Hadjidi S, Parashar VK, Vandevyver C, Rida A, Gijs MAM (2006) Two-dimensional magnetic manipulation of microdroplets on a chip as a platform for bioanalytical applications. *Sensors Actuators, B Chem.* 117(2):457–463
5. Guo ZG, Zhou F, Hao JC, Liang YM, Liu WM, Huck WTS (2006) ‘Stick and slide’ ferrofluidic droplets on superhydrophobic surfaces. *Appl Phys Lett* 89(8):1–4
6. Renaudin A, Tabourier P, Camart JC, Druon C (2006) Surface acoustic wave two-dimensional transport and location of microdroplets using echo signal. *J Appl Phys* 100(11):1–4
7. Guttenberg Z et al (2005) Planar chip device for PCR and hybridization with surface acoustic wave pump. *Lab Chip* 5(3):308–317
8. Hunt TP, Issadore D, Westervelt RM (2008) Integrated circuit/microfluidic chip to programmably trap and move cells and droplets with dielectrophoresis. *Lab Chip* 8(1):81–87
9. Velev OD, Prevo BG, Bhatt KH (2003) On-chip manipulation of free droplets. *Nature* 426(6966):515–516
10. Pollack MG, Fair RB, Shenderov AD (2000) Electrowetting-based actuation of liquid droplets for microfluidic applications. *Appl Phys Lett* 77(82):1725–1726
11. Fair RB (2007) Digital microfluidics: Is a true lab-on-a-chip possible? *Microfluid. Nanofluidics* 3(3):245–281
12. Pei SN, Valley JK, Neale SL, Jamshidi A, Hsu HL, Wu MC (2010) Light-actuated digital microfluidics for large-scale, parallel manipulation of arbitrarily sized droplets. In: Proceedings of IEEE international conference on mMicro electro mechanical systems, pp 252–255
13. Chiou PY, Moon H, Toshiyoshi H, Kim CJ, Wu MC (2003) Light actuation of liquid by optoelectrowetting. *Sensors Actuators, A Phys.* 104(3):222–228
14. Mugele F, Baret J-C (2005) Electrowetting: from basics to applications. *J Phys: Condens Matter* 17(28):R705–R774
15. Berthier J (2008) Microdrops and digital microfluidics
16. Berthier J et al (2005) An analytical model for the prediction of microdrop extraction and splitting in digital microfluidics systems. In: 2005 NSTI Nanotechnology conference trade show—NSTI nanotechnology 2005 technical proceedings, vol 1, no c, pp 664–667
17. Kang KH (2002) How electrostatic fields change contact angle in electrowetting. *Langmuir* 18(26):10318–10322
18. Jebrail MJ et al (2014) A solvent replenishment solution for managing evaporation of biochemical reactions in air-matrix digital microfluidics devices. *Lab Chip* 15(1):151–158
19. Yi U-C, Kim C-J (2006) Characterization of electrowetting actuation on addressable single-side coplanar electrodes. *J Micromech Microeng* 16(16):2053–2059
20. Malic L, Brassard D, Veres T, Tabrizian M (2010) Integration and detection of biochemical assays in digital microfluidic LOC devices. *Lab Chip* 10(4):418–431
21. Srinivasan V, Pamula VK, Fair RB (2004) Droplet-based microfluidic lab-on-a-chip for glucose detection. *Anal Chim Acta* 507(1):145–150
22. Srinivasan V, Pamula VK, Fair RB (2004) An integrated digital microfluidic lab-on-a-chip for clinical diagnostics on human physiological fluids. *Lab Chip* 4(4):310–315
23. Norian H, Field RM, Kymissis I, Shepard KL (2014) An integrated CMOS quantitative-polymerase-chain-reaction lab-on-chip for point-of-care diagnostics. *Lab Chip* 14(20):4076–4084

24. Kühnemund M, Witters D, Nilsson M, Lammertyn J (2014) Circle-to-circle amplification on a digital microfluidic chip for amplified single molecule detection. *Lab Chip* 14(16):2983–2992
25. Sista R et al (2008) Development of a digital microfluidic platform for point of care testing. *Lab Chip* 8(12):2091
26. Luan L, Evans RD, Jokerst NM, Fair RB (2008) Integrated optical sensor in a digital microfluidic platform. *IEEE Sens J* 8(5):628–635
27. Miller EM, Ng AHC, Uddayasankar U, Wheeler AR (2011) A digital microfluidic approach to heterogeneous immunoassays. *Anal Bioanal Chem* 399(1):337–345
28. Malic L, Veres T, Tabrizian M (2011) Nanostructured digital microfluidics for enhanced surface plasmon resonance imaging. *Biosens Bioelectron* 26(5):2053–2059
29. Sarkar PK, Prajapati PK, Shukla VJ, Ravishankar B, Choudhary AK (2015) Advances in coupling microfluidic chips to mass spectrometry. *Mass Spectrom Rev* 34:535–557
30. Hu J-B, Chen T-R, Chang C-H, Cheng J-Y, Chen Y-C, Urban PL (2015) A compact 3D-printed interface for coupling open digital microchips with Venturi easy ambient sonic-spray ionization mass spectrometry. *Analyst* 140(5):1495–1501
31. Han KN, Li CA, Seong GH (2013) Microfluidic chips for immunoassays. *Annu. Rev. Anal. Chem.* 6:119–141
32. Jebrail MJ, Bartsch MS, Patel KD (2012) Digital microfluidics: a versatile tool for applications in chemistry, biology and medicine. *Lab Chip* 12(14):2452–2463
33. Yu Y, Chen J, Zhou J (2014) Parallel-plate lab-on-a-chip based on digital microfluidics for on-chip electrochemical analysis. *J Micromech Microeng* 24(1):15020
34. Choi K, Kim J-Y, Ahn J-H, Choi J-M, Im M, Choi Y-K (2012) Integration of field effect transistor-based biosensors with a digital microfluidic device for a lab-on-a-chip application. *Lab Chip* 12(8):1533–1539
35. Samiei E, Luka GS, Najjaran H, Hoorfar M (2016) Integration of biosensors into digital microfluidics: impact of hydrophilic surface of biosensors on droplet manipulation. *Biosens Bioelectron* 81:480–486
36. Nejad HR, Samiei E, Ahmadi A, Hoorfar M (2015) Gravity-driven hydrodynamic particle separation in digital microfluidic systems. *RSC Adv* 5(45):35966–35975
37. Zhou Y, Li B, Wang M, Yang Z, Yin H, Ai S (2014) Enzyme-based electrochemical biosensor for sensitive detection of DNA demethylation and the activity of DNA demethylase. *Anal Chim Acta* 840:28–32
38. Amine A, Arduini F, Moscone D, Palleschi G (2016) Recent advances in biosensors based on enzyme inhibition. *Biosens Bioelectron* 76:180–194
39. Lin H, Zhang W, Jia S, Guan Z, Yang CJ, Zhu Z (2014) Microfluidic approaches to rapid and efficient aptamer selection. *Biomicrofluidics* 8(4):41501
40. Jia X, Dong S, Wang E (2016) Engineering the bioelectrochemical interface using functional nanomaterials and microchip technique toward sensitive and portable electrochemical biosensors. *Biosens Bioelectron* 76:80–90
41. Vergauwe N et al (2011) A versatile electrowetting-based digital microfluidic platform for quantitative homogeneous and heterogeneous bio-assays. *J Micromech Microeng* 21:54026
42. Samiei E, Hoorfar M (2015) Systematic analysis of geometrical based unequal droplet splitting in digital microfluidics. *J Micromech Microeng* 25:55008
43. Lin Y, Welch ERF, Fair RB (2012) Low voltage picoliter droplet manipulation utilizing electrowetting-on-dielectric platforms. *Sens Actuators B Chem* 173:338–345
44. Lin Y, Evans RD, Welch E, Hsu B, Madison AC, Fair RB (2010) Low voltage electrowetting-on-dielectric platform using multi-layer insulators. *Sens Actuators B Chem* 150(1):465–470
45. Fobel R, Kirby AE, Ng AHC, Farnood RR, Wheeler AR (2014) Paper microfluidics goes digital 2838–2843
46. Gong J, Kim C (2008) Direct-referencing two-dimensional-array digital microfluidics using multilayer printed circuit board. *J Microelectromech Syst* 17(2):257–264
47. Sista RS et al (2013) Multiplex newborn screening for Pompe, Fabry, Hunter, Gaucher, and Hurler diseases using a digital microfluidic platform. *Clin Chim Acta* 424:12–18

48. Mohamed Y, Saurabh S, Homayoun N (2015) Fabrication of digital microfluidic devices on flexible paper-based and rigid substrates via screen printing. *J Micromech Microeng* 25(5):57001
49. Zeng X et al (2013) Chemiluminescence detector based on a single planar transparent digital microfluidic device. *Lab Chip* 13(14):2714–2720
50. Ko H et al (2014) Active digital microfluidic paper chips with inkjet-printed patterned electrodes. *Adv Mater* 26(15):2335–2340
51. Moon H, Cho SK, Garrell RL, Kim CJ (2002) Low voltage electrowetting-on-dielectric. *J Appl Phys* 92(7):4080–4087
52. Cho SK, Moon H, Kim CJ (2003) Creating, transporting, cutting, and merging liquid droplets by electrowetting-based actuation for digital microfluidic circuits. *J. Microelectromech Syst* 12(1):70–80
53. Foudeh AM, Brassard D, Tabrizian M, Veres T (2015) Rapid and multiplex detection of Legionella's RNA using digital microfluidics. *Lab Chip* 15(6):1609–1618
54. Li Y et al (2008) Anodic Ta₂O₅ for CMOS compatible low voltage electrowetting-on-dielectric device fabrication. *Solid State Electron* 52(9):1382–1387
55. Dong C et al (2015) On the droplet velocity and electrode lifetime of digital microfluidics: voltage actuation techniques and comparison. *Microfluid Nanofluid* 18(4):673–683
56. Brassard D, Malic L, Normandin F, Veres T, Tabrizian M (2008) Water-oil core-shell droplets for electrowetting-based digital microfluidic devices. *Lab Chip* 8(8):1342–1349
57. Nestor BA et al (2016) Digital microfluidic platform for dielectrophoretic patterning of cells encapsulated in hydrogel droplets. *RSC Adv* 6(62):57409–57416
58. Gong J, Kim C-JCJ (2008) All-electronic droplet generation on-chip with real-time feedback control for EWOD digital microfluidics. *Lab Chip* 8(6):898–906
59. Liu Y, Banerjee A, Papautsky I (2014) Precise droplet volume measurement and electrode-based volume metering in digital microfluidics. *Microfluid. Nanofluid* 17(2): 295–303
60. Paik P, Pamula VK, Fair RB (2003) Rapid droplet mixers for digital microfluidic systems. *Lab Chip* 3(4):253–259
61. Samiei E, Diaz de Leon Derby M, van den Berg A, Hoorfar M (2016) An electrohydrodynamic technique for rapid mixing in stationary droplets on digital microfluidic platforms. *Lab Chip*
62. Tsaloglou MN, Jacobs A, Morgan H (2014) A fluorogenic heterogeneous immunoassay for cardiac muscle troponin cTnI on a digital microfluidic device. *Anal Bioanal Chem* 406(24):5967–5976
63. Ng AHC, Lee M, Choi K, Fischer AT, Robinson JM, Wheeler AR (2015) Digital microfluidic platform for the detection of rubella infection and immunity: A proof of concept. *Clin Chem* 61(2):420–429
64. Samiei E, Rezaei Nejad H, Hoorfar M (2015) A dielectrophoretic-gravity driven particle focusing technique for digital microfluidic systems. *Appl Phys Lett* 106(20):204101
65. Li Z, Ho TY, Chakrabarty K (2014) Optimization of heaters in a digital microfluidic biochip for the polymerase chain reaction. In: 2014—20th International Workshop on Thermal. Investigation of ICs and Systems Proceedings (THERMINIC), vol. 2014, pp. 1–5
66. Krishnan S, Weinman CJ, Ober CK (2008) Advances in polymers for anti-biofouling surfaces. *J Mater Chem* 18:3405
67. Patel P, Choi CK, Meng DD (2010) Superhydrophilic Surfaces for Antifogging and Antifouling Microfluidic Devices. *JALA J Assoc Lab Autom* 15(2):114–119
68. Yoon JY, Garrell RL (2003) Preventing biomolecular adsorption in electrowetting-based biofluidic chips. *Anal Chem* 75(19):5097–5102
69. Luk VN, Mo GC, Wheeler AR (2008) Pluronic additives: a solution to sticky problems in digital microfluidics. *Langmuir* 24(12):6382–6389
70. Yang H, Luk VN, Abalgawad M, Barbulovic-nad I, Wheeler AR (2009) A world-to-chip interface for digital microfluidics. *Anal Chem* 81(December 2008):1061–1067

71. P. Bayiati, A. Tserepi, P. S. Petrou, S. E. Kakabakos, K. Misiakos, and E. Gogolides, "Electrowetting on plasma-deposited fluorocarbon hydrophobic films for biofluid transport in microfluidics," *J. Appl. Phys.*, vol. 101, no. 10, 2007
72. Prakash R, Papageorgiou DP, Papathanasiou AG, Kaler KVIS (2013) Dielectrophoretic liquid actuation on nano-textured super hydrophobic surfaces. *Sens Actuators B Chem* 182:351–361
73. Myers FB, Lee LP (2008) Innovations in optical microfluidic technologies for point-of-care diagnostics. *Lab Chip* 8(12):2015–2031
74. Bender BF, Aijian AP, Garrell RL (2016) Digital microfluidics for spheroid-based invasion assays. *Lab Chip* 16(8):1505–1513
75. Chang YH, Bin Lee G, Huang FC, Chen YY, Lin JL (2006) Integrated polymerase chain reaction chips utilizing digital microfluidics. *Biomed Microdevices* 8(3):215–225
76. Kumar PT et al (2015) Digital microfluidics for time-resolved cytotoxicity studies on single non-adherent yeast cells. *Lab Chip* 15(8):1852–1860
77. Sista RRS, Eckhardt AEA, Srinivasan V, Pollack MG, Palanki S, Pamula VK (2008) Heterogeneous immunoassays using magnetic beads on a digital microfluidic platform. *Lab Chip* 8(12):2188–2196
78. Kirby AE, Lafrenière NM, Seale B, Hendricks PI, Cooks RG, Wheeler AR (2014) Analysis on the go: quantitation of drugs of abuse in dried urine with digital microfluidics and miniature mass spectrometry. *Anal Chem* 86(12):6121–6129
79. Shih SCC et al (2012) Dried blood spot analysis by digital microfluidics coupled to nano-electrospray ionization mass spectrometry. *Anal Chem* 84(8):3731–3738
80. Fouillet Y, Jary D, Chabrol C, Claustre P, Peponnet C (2008) Digital microfluidic design and optimization of classic and new fluidic functions for lab on a chip systems. *Microfluid Nanofluid* 4(3):159–165
81. Zeng Z, Zhang K, Wang W, Xu W, Zhou J (2016) Portable Electrowetting Digital Microfluidics Analysis Platform For Chemiluminescence Sensing. *IEEE Sens J* 16(11):4531–4536
82. Shamsi MH, Choi K, Ng AHC, Dean Chamberlain M, Wheeler AR (2016) Electrochemiluminescence on digital microfluidics for microRNA analysis. *Biosens Bioelectron* 77:845–852
83. Malic L, Veres T, Tabrizian M (2009) Two-dimensional droplet-based surface plasmon resonance imaging using electrowetting-on-dielectric microfluidics. *Lab Chip* 9(3):473–475
84. Malic L, Veres T, Tabrizian M (2009) Biochip functionalization using electrowetting-on-dielectric digital microfluidics for surface plasmon resonance imaging detection of DNA hybridization. *Biosens Bioelectron* 24(7):2218–2224
85. Shamsi MH, Choi K, Ng AHC, Wheeler AR (2014) A digital microfluidic electrochemical immunoassay. *Lab Chip* 14(3):547–554
86. Rackus DG et al (2015) A digital microfluidic device with integrated nanostructured microelectrodes for electrochemical immunoassays. *Lab Chip* 15(18):3776–3784
87. Mok J, Mindrinos MN, Davis RW, Javanmard M (2014) Digital microfluidic assay for protein detection. *Proc Natl Acad Sci* 111(6):2110–2115